ORIGINAL ARTICLE

Performance Investigation of a Three Fluid Heat Exchanger Used in Domestic Heating Applications

Taraprasad Mohapatra[1], Sudhansu S. Sahoo[2,*], Sudhansu S. Mishra[3], Prasheet Mishra[1], Dillip K. Biswal[1]

[1]Department of Mechanical Engineering, C. V. Raman Global University, Bhubaneswar 752054, India
[2]Department of Mechanical Engineering, Odisha University of Technology and Research, Bhubaneswar 751029, India
[3]Department of Mechanical Engineering, Government College of Engineering, Keonjhar 758002, India

ABSTRACT – Recent work analytically investigates the heat transfer characteristics of a three fluid heat exchanger used for domestic heating applications with respect to different design parameters, i.e. flow rate, inlet temperature, tube diameter, coil diameter, and coil pitch. The present and previous results are compared with the literature. Overall agreement among these results are observed with little variation. Afterwards, the present temperature data was verified with prior experimental data and little deviation observed in these results vary from -4.28 % to +6.68 % and -6.17% to +5.92% in parallel and counter flow configuration, respectively. It is ensued that the coil side Nusselt number increases with the rise in coil side fluid flow rate and inlet temperature, coil outside fluid inlet temperature and coil diameter respectively. The increment in coil side flow rate and inlet temperature are identified as the major contributors, with 297% and 39.5% contributions. Similarly, growth in coil outside Nusselt number is observed with the rise in coil side fluid inlet temperature and flow rate, coil outside fluid flow rate and inlet temperature, and coil pitch respectively. The coil pitch and flow rate at the coil outside are identified as major contributors with 36% and 28.5% contribution repsectively. Distinct correlations for heat transfer in the present HEx are proposed for coil inside and outside fluid flow in a turbulent flow regime. The developed correlations results are compared with the present result, and reasonable agreement is observed within the data range of +13% to -14% and +10% to -11% for coil inside and outside Nusselt number, respectively.

NOMENCLATURE

A	Area, m^2		ε	Effectiveness
c	Specific heat, kJ/kg-K		μ	viscosity, N-s/m^2
C	Heat capacity, kJ/K		δ	Curvature ratio, $\frac{d_{c,i}}{D_c}$
d	Diameter, m		*Subscripts*	
D_c	Diameter of helical coil, m		1	Inlet
D_e	Dean number, $De = Re.\sqrt{\frac{d_{c,i}}{D_c}}$		2	Outlet
D_{eq}	Equivalent diameter, m		act	Actual
HEx	Heat Exchanger		c	Coil
h	Convective heat transfer coefficient, W/ m^2.K		cr	Critical
k	Thermal conductivity, W/m-K		cu	Copper
L	Length , m		e	Equivalent
$\dot{m}$	Mass flow rate, kg/sec		i	Inner
N	Number of turns		im	Inmost tube
Nu	Nusselt number		if	The helical coil inside a fluid
p	Helical coil pitch, m		imf	Inmost tube side fluid
Pr	Prandtl number		I	Part-1 (Hot water to normal water)
$\dot{Q}$	Heat Transfer Rate, W		II	Part-2 (Normal water to air)
Re	Reynolds number		m	mean
T	Temperature, ºC		max	Maximum
U	Overall heat transfer co-efficient, W/m^2.K		min	Minimum
v	Velocity, m/sec		o	Outer
V	Volumetric flow rate, m^3/sec		oa	Outer Annulus
$\tilde{V}$	Volume, m^3		of	Helical coil outside fluid

Greek symbols		*TS*	Test section
ρ	Density, kg/m^3		

INTRODUCTION

Two fluid heat exchangers are commonly used HEx in which two fluid streams are flowing through two different passages separated by a wall. However, for some specific applications like liquefaction of gases, HVAC and food processing industries, and heat recovery process, three fluids HEx are used. Compared to two fluid HEx, three fluid HEx are more compact, occupy less space, and perform better. Thus, currently, several works on this research area, i.e. three fluid HEx are going on. All types of heat exchangers associated with three fluids are minutely reviewed and classified [1] according to heat transfer communications among fluids. A detailed procedure towards the preparation of a mathematical model using a dimensionless group was elaborated. Mathematical modeling with possible solution techniques for heat exchangers with three concentric tubes was explained [2], and several case studies were conducted [3]. A similar study was carried out [4] and [5] in two different sections for heat exchangers associated with three thermal interactions. In the first part, the modeling of the heat exchangers was elaborated mathematically for all arrangements of flow. In the second part, the performance of the heat exchangers is determined. A diary heat exchanger is modeled and simulated [6] for the measurement of the scaling effect and exit temperature of the milk.

It is noted from the results that mostly fouling occurs in the tubes towards the outlet. Temperature and shear stress are the main parameters which control the thickness of fouling observed. The heat transfer performance of a helical coil integrated heat exchanger for three fluids is determined experimentally [7]. Numerical analysis and performance optimization of three fluid heat exchangers are analyzed and found in the literature [8], [9]. The coefficient of convection heat transfer through the helical coil is calculated using Wilson plot method. The heating competence of the present heat exchanger is determined concerning flow direction and rate of mass transfer. A heat exchanger with the concentric helical coil is experimentally and numerically studied, and a heat transfer correlation is proposed [10]. A heat exchanger with the helical coil is studied [11] numerically and two correlations proposed; one for heat transfer and another is for friction factor. For better heat transfer among fluids, a tube with helical tape inserts is studied experimentally [12]. Fluid flow and heat transfer correlations were proposed for different tube inserts in the turbulent region. The thermo-fluid behavior of a triple tube heat exchanger is numerically studied [13] using the FORTRAN code. Solidification and melting of phase change material in a triplex concentric tube heat exchanger for thermal energy storage have been investigated [14] experimentally and numerically. The results of the numerical work were verified and validated with experimental work with good agreement. It has resulted that with the inlet fluid temperature at 23 °C, the solidification front radius of PCM at different axial position increases with increasing time. The time taken for complete solidification at the entrance, middle, and end of the tube is about 40, 50, and 100 min, respectively was observed. The PCM solidification in a triplex tube heat exchanger was numerically studied [15] with internal and external fins.

Different design parameters as heat transfer enhancement techniques, which included fin length, number of fins, fin thickness, and PCM unit geometry, were analyzed. It was observed that the effect of fin thickness was smaller than that of the fin length on the solidification of PCM. The thermo-fluidic performance of a triple tube heat exchanger was investigated experimentally and numerically [16] concerning different inserts. An increment of nearly 12% in overall heat transfer co-efficient and nearly 14.5% in effectiveness was observed for rib type inserts in both modes of investigation. A three-fluid heat exchanger used for cryogenic application with three thermal communications was investigated [17] to predict the effect of heat leak analytically and numerically. The behavior of the hot fluid, the temperature profile of different fluids, heat transfer effectiveness, and degradation factor were investigated concerning seven different non-dimensional parameters. Variation in different fluid temperatures along the length of a triple concentric pipe heat exchanger was investigated numerically [18]. The temperature data obtained from the finite element method (FEM) were compared with experimental data, and good agreement between them was observed. The effect of various design parameters on the temperature distributions was deliberated.

From the literature review, it is found that the performance investigation for various design parameters and heat transfer correlation development for fluid flow inside and outside of the helical coilin counterflow configuration in the present HEx is missing in the literature. Due to the complicated system and time-consuming process to obtain results, the use of heat transfer correlations is helpful for the design of effective HEx. With this motivation, heat transfer correlation development and the performance investigation for the present HExwith respect to various design parameters, i.e. flow rate, inlet temperature, tube diameter, coil diameter, and coil pitch, are intended in this study. For the stated objectives, the present HExis analytically modeled, results are compared, verified, validated, and investigated theoretically as it is rather a time taking and inexpensive to perform these performance tests experimentally. Afterwards, distinct correlations for heat transfer inner side and outer side of the helical coil were developed for more generic use by researchers and manufacturers.

MATERIALS AND METHOD

Experimental Method

A distinct method for daytime heating of air and water in a three fluid heat exchanger (TFHE) using solar thermal energy is shown in Figure 1. From Figure 1, it is acknowledged that the solar thermal energy absorbed in the solar flat plate collector by the heating fluid is utilized to heat incoming normal water and air inside the present HEx for domestic heating purposes. The heating fluid, i.e. hot water, normal water, and air, are being considered as the coil side, coil outside,

and inmost tube side fluid in the present work flowing through the helical coil tube, outermost straight tube, and inmost tube of the present HEx respectively. The present technique is proposed for domestic heating during the winter season and in cold regions of our country.
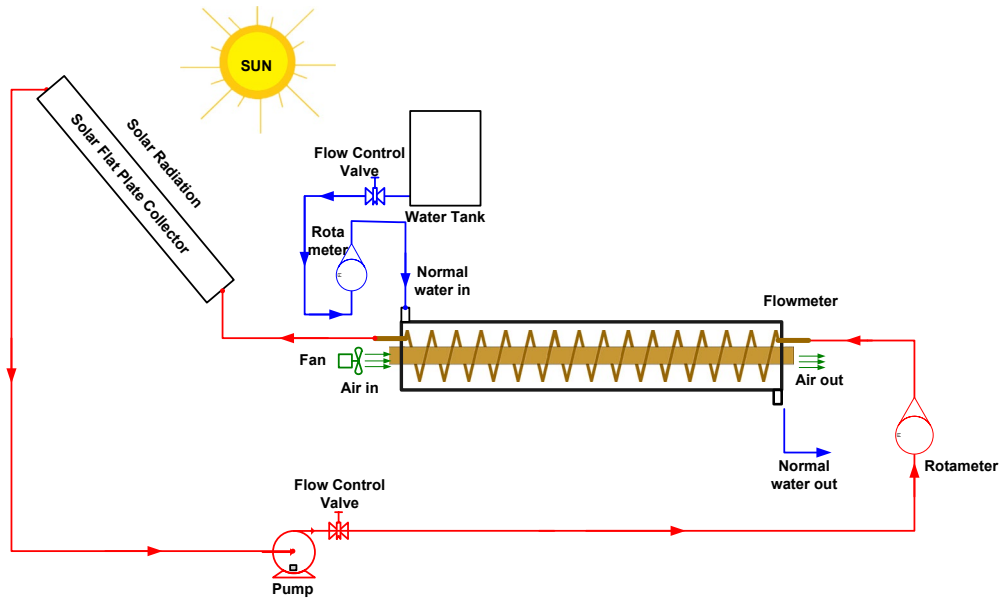
Figure 1. Schematic layout of the domestic heating system using solar thermal energy.

The thermal performance of the HEx illustrated in Figure 1 for domestic water and air heating was investigated experimentally [7]. Overall heat transfer coefficient and effectiveness of the HEx were determined as the performance parameters concerning variation in mass flow rate and inlet temperature of different fluids. The experimental setup investigated consists of a HEx test section insulated externally, a hot water tank with an immersion heater and thermostat, a pump, ball valves, flow control valves, Rotameters, blower, as shown in Figure 2. A 0.5 HP centrifugal pump was used to supply hot water from a tank equipped with an immersion heater and thermostat, normal water was supplied from an overhead tank, and air was supplied by a blower. To reduce experiment cost, the solar flat plate collector shown in Figure 1 was replaced by the hot water tank in the experimental setup for the same requirement of supplying hot water at a rated temperature. Rotameter was used to measure the volumetric flow rate of both hot and normal water. The error associated with volume flow rate measurement in the rotameter was determined ± 12.6 %. Ball valves were used to regulate the volumetric flow rate of hot water and normal water, whereas a flow control valve was used to control the air flow rate. The air velocity was measured by an anemometer. The error associated with air velocity measurement in the anemometer was determined at ± 3 %. 4 K-type thermocouples were used at four different locations of the test section for each fluid stream to measure inlet, two intermediate, and outlet temperatures. The error associated with temperature measurement in the rotameter was determined at ± 6.7 % for water and ±9.1 % for air. The uncertainties involved in performances were calculated at ± 15.06 % for the overall heat transfer coefficient and ± 14.89 % for heat transfer effectiveness.
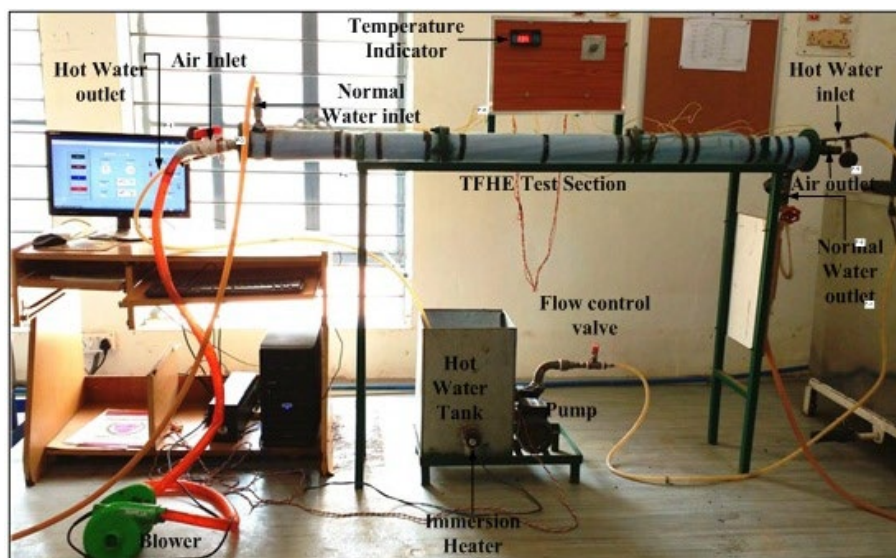
Figure 2. Experimental setup [7].

The Hex earlier tested is an improved version of the double pipe heat exchanger, where a helical coil is inserted between two concentric straight tubes for heat transfer enhancement among fluids. The details of the TFHE test section were used in [7], and its schematic layout is shown in Figure 3.
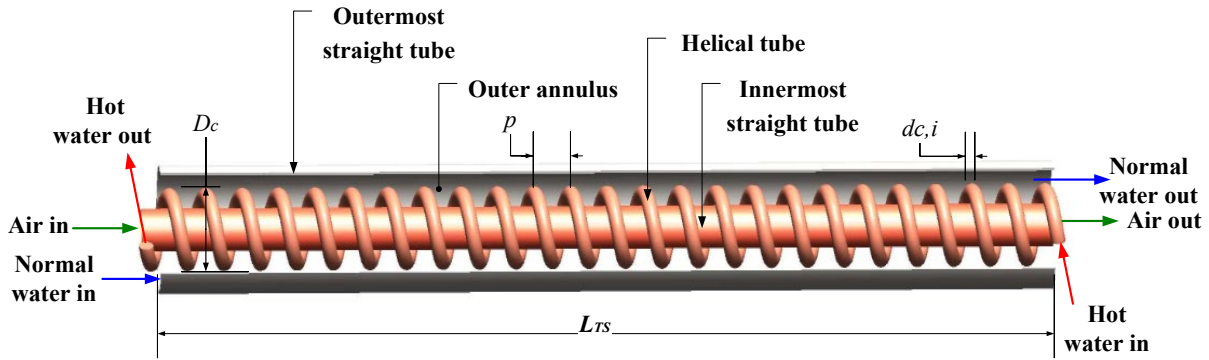

Figure 3. Configuration of TFHE test section.

The outermost straight tube made up of G.I. pipe, simply acts as a shell for fluid flow outside of the helical coil of 1.8 m length, 0.07 m internal diameter, and 0.0025 m thickness and insulated outside. The air passes through the inmost straight tube made up of copper of length 2.0 m, an internal diameter of 0.0045 m, and a thickness of 0.001 m. The helical coil is also made up of copper inserted in the outer annulus of two concentric straight tubes in such a way that the distances maintained from both of the straight tubes are the same. The length of the helical coil is 21.261 m, coil diameter is 0.0494 m, the pitch is 0.013 m, 137 turns, inside diameter is 0.0045 m, curvature ratio is 0.1315, and pitch to inside diameter ratio is 2.88. The above-said dimensions are also used in the formulation of the analytical model.

The theoretical model of the TFHE is prepared using the above-mentioned geometrical data and different fluid temperatures at the outlet of the TFHE are determined analytically. The analytical modeling and technique used to determine the outlet temperatures of fluids using the control volume approach are explained below.

Analytical Modeling

In this study, the heating performance of the TFHE and heat transfer correlation development are conducted in an analytical model. The control volume method and some commonly used empirical formulas are used in the preparation of the analytical model. In the following sections, detailed information about these formulas and the control volume approach is presented.

Average temperature

The average temperature of fluid flow inside the helical coil,

$$T_{if,m} = \frac{T_{if,1} + T_{if,2}}{2} \tag{1}$$

The average temperature of fluid flow outside helical coil,

$$T_{of,m} = \frac{T_{of,1} + T_{of,2}}{2} \tag{2}$$

The average temperature of fluid flow inside the inmost tube,

$$T_{imf,m} = \frac{T_{imf,1} + T_{imf,2}}{2} \tag{3}$$

Rate of mass flow

Rate of mass flow inside the helical coil,

$$\dot{m}_{if} = \rho_{if}.V_{if} \tag{4}$$

Rate of mass flow outside the helical coil,

$$\dot{m}_{of} = \rho_{of}.V_{of} \tag{5}$$

Rate of mass flow inside the inmost tube,

$$\dot{m}_{imf} = \rho_{imf}.V_{imf} \tag{6}$$

Heat transfer rate

Rate of heat transfer from fluid flowing inside the helical coil,

$$\dot{Q}_{if} = \dot{m}_{if} . c_{if} . (T_{if,1} - T_{if,2}) \tag{7}$$

The heat transfer rate to fluid flowing outside of the helical coil,

$$\dot{Q}_{of} = \dot{m}_{of} . c_{of} . (T_{of,2} - T_{of,1}) \tag{8}$$

The heat transfer rate to fluid flowing through the inmost tube,

$$\dot{Q}_{imf} = \dot{m}_{imf} . c_{imf} . (T_{imf,2} - T_{imf,1}) \tag{9}$$

Reynolds number

Reynolds number for fluid flow inside of the helical coil,

$$Re_{if} = \frac{\rho_{if} . v_{if} . d_{c,i}}{\mu_{if}} \tag{10}$$

Reynolds number for fluid flow outside of the helical coil,

$$Re_{of} = \frac{\rho_{of} . v_{of} . D_{eq}}{\mu_{of}} \tag{11}$$

Reynolds number for fluid flow inside the inmost tube,

$$Re_{imf} = \frac{\rho_{imf} . v_{imf} . d_{im,i}}{\mu_{imf}} \tag{12}$$

Critical Reynolds number [19] for fluid flow inside of the helical coil,

$$Re_{cr} = 2 \times 10^4 \times \left(\frac{d_{c,i}}{D_c}\right)^{0.32} \tag{13}$$

Nusselt number

Nusselt number of fluid flow inside the helical coil, Nu_{if} is calculated from the following correlations provided [16].

$$Nu_{if} = 0.913D\, e^{0.476}\, Pr^{0.2} \quad \text{for } 0.01 \le \delta \le 0.1, 80 \le D\,e \le 1{,}200 \text{ and } 0.7 \le Pr \le 5 \tag{14}$$

$$Nu_{if} = 0.836D\, e^{0.5}\, Pr^{0.1} \quad \text{for } 0.01 \le \delta \le 0.1, D\,e \ge 1{,}200 \text{ and } 0.7 \le Pr \le 5 \tag{15}$$

where De is the Dean number. It signifies the effect of viscous force on centrifugal force for fluid flow in a curved tube or helical tube. Nusselt number of the fluid flowing outer side of the helical coil, Nu_{of} is estimated from the following correlation provided by [15].

$$Nu_{of} = 0.6R\, e^{0.5}\, Pr^{0.31} \quad \text{for } 50 \le Re_{of} \le 10{,}000 \tag{16}$$

Nusselt number of fluid flow in the inmost tube, Nu_{imf} is calculated from Gnielinski's [18] correlation.

$$Nu_{imf} = 0.0214 \left(Re_{imf}^{0.8} - 100 \right) Pr^{0.4} \left(1 + \left(\frac{d_{im}}{L_{im}}\right)^{\frac{2}{3}} \right) \text{ for } 0.5 < Pr < 1.5, 2300 < Re_{imf} < 10^6 \text{ and } 0 < \frac{d_{im}}{L_{im}} < 1 \tag{17}$$

Heat transfer coefficients

Coefficient of heat transfer for fluid flow through the helical coil,

$$h_{if} = \frac{Nu_{if}K_{if}}{d_{c,i}} \tag{18}$$

Coefficients of heat transfer for fluid flowing outside of the helical coil,

$$h_{of} = \frac{Nu_{of}K_{of}}{D_{eq}} \tag{19}$$

Coefficients of heat transfer of fluid flowing through the inmost tube,

$$h_{imf} = \frac{Nu_{imf}K_{imf}}{d_{im,i}} \tag{20}$$

Overall heat transfer coefficient

In this study, two overall heat transfer coefficients have been calculated for heat transfer from helical coil side fluid to fluid flowing outside of the helical coil as well as for heat transfer from helical coil outside fluid to fluid flowing through the inmost tube. For the transfer of heat energy from fluid flowing through the inner side of the helical coil to fluid flowing outside of the helical coil, the overall heat transfer coefficient is assessed using the following formula.

$$\frac{1}{U_{o,I}} = \frac{d_{c,o}}{h_{if}.d_{c,i}} + \frac{A_{c,o}.\ln\left(\frac{d_{c,o}}{d_{c,i}}\right)}{2\pi K_{cu}L_c} + \frac{1}{h_{of}} \tag{21}$$

For the transfer of heat energy from fluid flowing outside of the helical coil to fluid flowing through the inmost tube, the overall heat transfer coefficient is evaluated using the following formula.

$$\frac{1}{U_{o,II}} = \frac{d_{im,i}}{h_{of}.d_{im,o}} + \frac{A_{im,i}.\ln\left(\frac{d_{im,i}}{d_{im,o}}\right)}{2\pi.K_{cu}.L_{TS}} + \frac{1}{h_{imf}} \tag{22}$$

Effectiveness

Heat transfer effectiveness in heat exchanger is calculated by:

$$\varepsilon = \frac{\dot{Q}_{act}}{\dot{Q}_{max}} \tag{23}$$

For energy transfer from fluid flow inside of the helical coil to fluid flow outside of the helical coil,

$$\dot{Q}_{act} = C_{if}\left(T_{if,1} - T_{if,2}\right) \tag{24}$$

$$\dot{Q}if, 1_{of,1} min_{max} \tag{25}$$

For energy transfer from fluid flowing outside of the helical coilto fluid flowing through the inmost tube,

$$\dot{Q}_{act} = C_{imf}\left(T_{imf,2} - T_{imf,1}\right) \tag{26}$$

$$\dot{Q}of, 1_{imf,1} min_{max} \tag{27}$$

Geometrical parameters [24]

Helical coil length for N numbers of turns,

$$L_c = N \times \sqrt{(\pi.D_c)^2 + (p)^2} \tag{28}$$

Helical coil volume,

$$\tilde{V}_c = \left(\frac{\pi}{4}\right).d_{c,o}{}^2.L_c \tag{29}$$

Shell side volume at the outer annulus side of a helical coil,

$$\tilde{V}_{oa} = \left(\frac{\pi}{4}\right) . \left(d_{om,i}{}^2 - d_{im,o}{}^2\right) p . N \tag{30}$$

Volume available for outer annulus side fluid flow,

$$\tilde{V}_{of} = \left(\tilde{V}_{oa} - \tilde{V}_c\right) \tag{31}$$

Equivalent diameter,

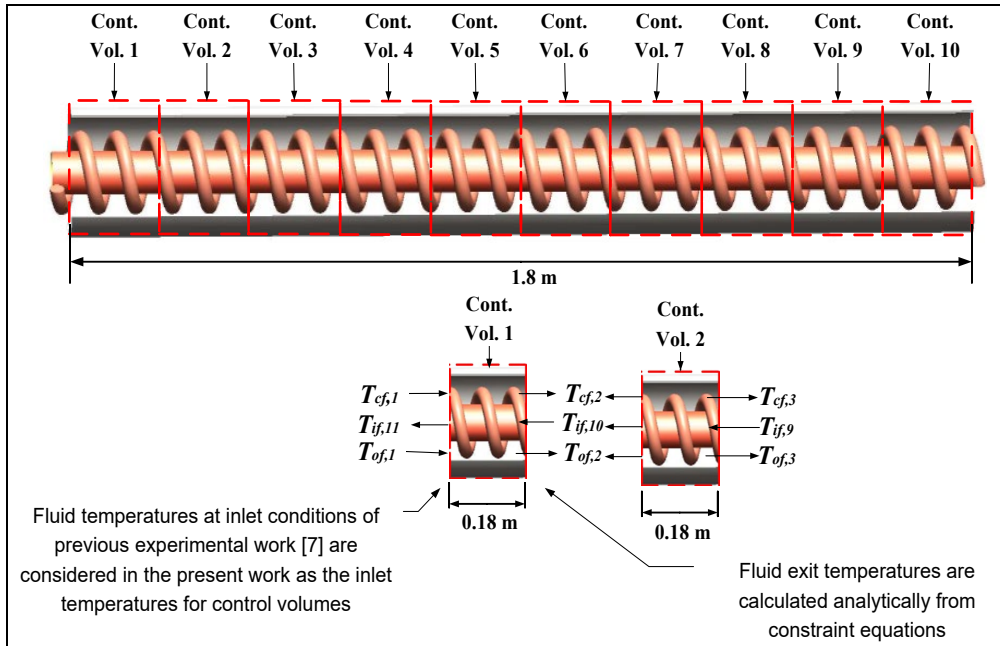$$D_{eq} = \frac{4 \times \tilde{V}_{of}}{\pi . d_{c,o} . L_c} \tag{32}$$

Figure 4. Determination of fluid temperature at the outlet of the heat exchanger using the control volume method.

Control volume technique and calculation of fluids outlet temperature

In the recent study, the control volume (CV) technique is used to predict the fluids outlet temperatures at the exit of the present HEx.The volume of the heat exchanger is allocated into ten separate control volumes, and the length of each CV is 0.18 m, as shown in Figure4. The fluids entering temperature, i.e. $T_{if,1}$=62.5 $^\circ$C, $T_{of,1}$=32°C, and $T_{imf,1}$= 35 °C, are considered in the analysis are the same as those taken in previous work [7]. The fluids outlet temperature, i.e. $T_{if,2}$, $T_{of,2,}$ and $T_{imf,2}$ at the exit of the control volume are determined using a solver with four constraint equations, Newton-Raphson method with iterations of 100, convergences of 0.0001, and tolerances of 5% with following assumptions and limitations.

Assumptions

   i.   Fluid flow is steady and incompressible.
   ii.   There are no phase changes that take place for fluid flow inside the HEx.
   iii.   Fluid properties are assumed to be constant concerning the variation of temperature.
   iv.   Thermal radiation heat transfer is small and has been neglected.
   v.   No heat transfer takes place from the present HEx to the external surrounding.

Limitations

   i.   The working pressure of the present heat exchanger is limited.
   ii.   Series heat transfer inside the present HEx in two stages from hot water to normal water and then from normal water to air limits the performance.

Following constraint equations[23] are used in this study. Heat rejected from fluid flow inside helical coil is equal to the heat absorbed by fluids flowing outside of the helical coil and inmost tube i.e.

$$\dot{Q}_{if} = \dot{Q}_{of} + \dot{Q}_{imf}$$
$$\Rightarrow \dot{m}_{if}.c_{p,if}.(T_{if,1} - T_{if,2}) = \dot{m}_{of}.c_{p,of}.(T_{of,2} - T_{of,1}) + \dot{m}_{imf}.c_{p,imf}.(T_{imf,2} - T_{imf,1}) \tag{33}$$

Heat rejected by fluid flowing through the helical coil is compared by following two different formulas.

$$\dot{Q}_{if} = \dot{Q}_{if}$$
$$\Rightarrow \dot{m}_{if}.c_{p,if}.(T_{if,1} - T_{if,2}) = \varepsilon.C(T_{if,1} - T_{of,1})_{min} \tag{34}$$

Heat transfer effectiveness is compared in counterflow arrangement [19].

$$\Rightarrow \left(\frac{\dot{m}_{if}.c_{p,if}.(T_{if,1} - T_{if,2})}{C_{min}.(T_{if,1} - T_{of,1})} \right) = \frac{1 - \exp(-NTU(1 - (C_{min}/C_{max})))}{1 - ((C_{min}/C_{max}).\exp(-NTU(1 - (C_{min}/C_{max}))))} \tag{35}$$

Subsequently, the outlet temperature of three fluids is determined from the CV 1 for three different input temperatures and above said conditions used in the solver. Afterwards, these outlet temperatures of fluids of CV 1 are used as the input temperatures in CV 2. Likewise, the outlet temperatures of fluids at the TFHE outlet are calculated by successive determination of the exit temperature for remaining control volumes, similar procedure adopted for the CV 1.

Log-Linear Regression Analysis

These analyses are generally carried out in a log-linear model to predict the exponential growth behavior of dependent variable (Y) concerning independent variables (X). These vastly used mathematical models are described by the following functional form:

$$Y_i = X_{1i}^{\beta_1} X_{2i}^{\beta_2} \ldots . X_{ki}^{\beta_k} e^{\in_i}$$
$$Y_i = X_{1i}^{\beta_1} X_{2i}^{\beta_2} \ldots . X_{ki}^{\beta_k} e^{\in_i} \tag{36}$$

In these models, dependent variables (Y) are a product of independent variables (X). $\beta_1, \beta_2 \ldots \beta_k$ are coefficient terms, $\in$ is the error term. These models can be easily transformed into linear models by taking the logarithmic of both sides of the equation (38). In the present study, the Nusselt number inside and outside of the helical coil is considered as the independent variable and calculated using a Log-linear regression model for various independent variables, i.e. fluid flow rates, tube diameter, coil pitch in counter flow arrangement.

Comparison and Validation

Figure 5 represents the comparison of results of the present work and prior experimental work [7] with the literature [20], [21], [22] for helical coil inside fluid Nusselt Number, Nu_{if} concerning variation in helical coil inside fluid Reynolds number for a range of 10000 – 50000. The results are calculated for a helical coil tube diameter of 0.0045 m, coil diameter of 0.0494 m, and pitch of 0.013 m. The results obtained by Nusselt number correlations provided by Seban McLaughlin [20], Roger and Mayhew [21], and Schimidt et al. [22] agreed with present and prior experimental work [7]. However, certain variations in results are observed, may be due to the dissimilar HEx geometry, thermal communication, flow arrangements, and boundary conditions.

Figure 6(a) and 6(b) represent the lengthwise distribution of fluid temperature in the current HEx. Both experimental [7] and analytical temperature data are plotted in Figure 6(a) and 6(b) for different flow arrangements. Temperature data obtained from previous experimental work [7] are compared and agreed with the current temperature data predicted analytically. The difference in temperature data varies from 0 to -4.28 % for hot water, 0 to -2.18 % for normal water, and 0 to +6.68% for air in parallel flow configuration. Similarly, the deviation in both temperature data is observed to be varying from +5.92 % to -4.42 % for hot water, 0 to -6.17 % for normal water, and 0 to +4.83% for air in counterflow configuration. Afterwards, the present analytical model was validated for these agreed temperature data but noticed quantitative deviation in results may be due to the errors associated with the instruments used in experiments.
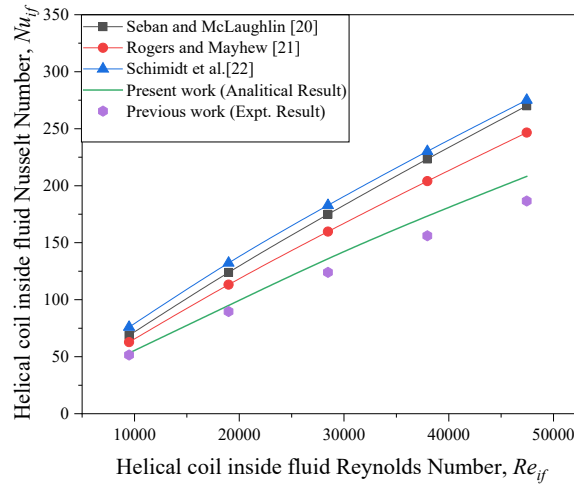
Figure 5. Comparison of the helical coil inside fluid Nusselt Number with literature.
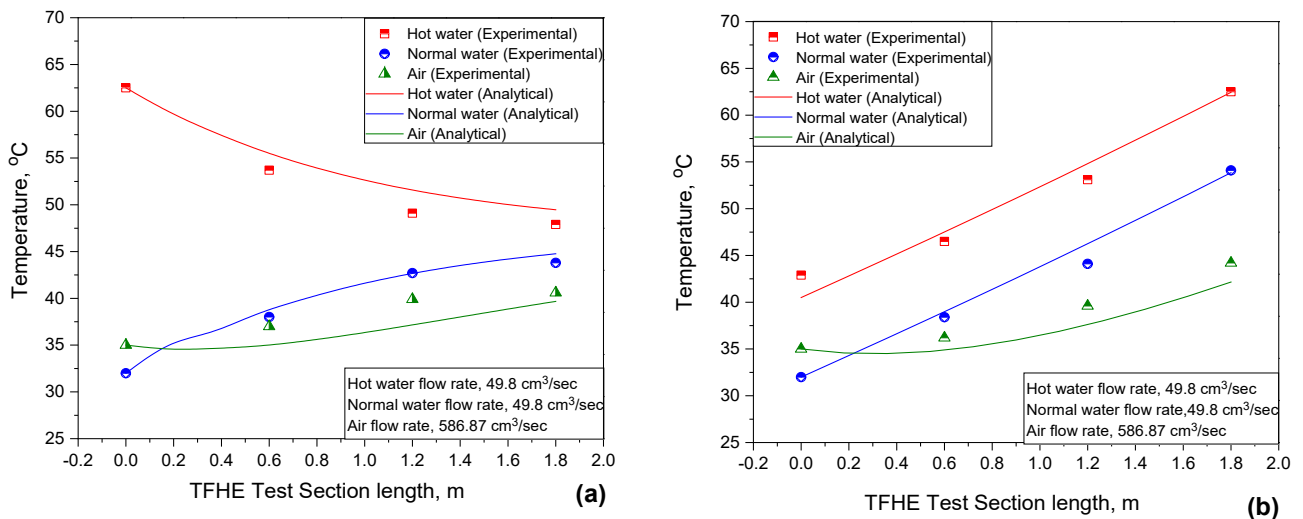

Figure 6. Validation of (a) co-current flow (b) counter current flow.

RESULTS AND DISCUSSION

The three fluid heat exchanger presented in this work is solely developed for domestic heating applications to supply hot water and air simultaneously. Hence, enhanced heating performance from the present HEx is always anticipated. Effective heat transfer from helical coil inside fluid i.e. hot water, will appreciably increase the temperatures of fluid flow at the outer side of the helical coil i.e. normal water and inmost straight tube side fluid i.e. air. However, these performances are affected by fluid types, flow parameters, and geometrical parameters associated with the current HEx. In the present work, the effect of different input parameters on heat transfer characteristics of the HEx is analyzed and discussed in counter flow direction for coil side fluid. Afterwards, correlations for estimation of coil side and outer annulus side Nusselt number are presented and validated against analytical results.

Effect of fluid flow rate at the inside of helical coil on heat transfer

The heating performance i.e. helical coil inside Nusselt number, $Nu_{if,}$ and outside Nusselt number, Nu_{of} of the current HEx are evaluated concerning variation in volume flow rate of the helical coil inside fluid i.e. 1 LPM, 3 LPM & 5 LPM successively. The result of this study is represented graphically in Figure7 for counter flow arrangement. It ensures that the helical coil inside Nusselt number, Nu_{if} increases considerably and outside Nusselt number, Nu_{of} inceases marginally with the rise in fluid flow rate inside of the helical coil.
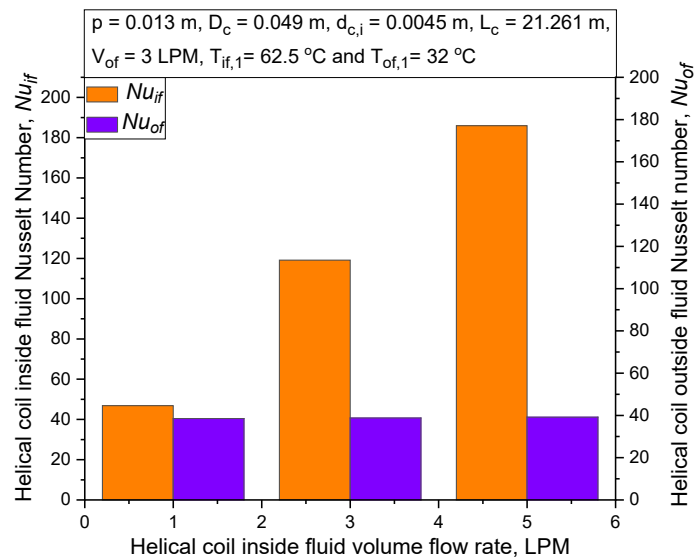
Figure 7. Effect of fluid flow rate at the inside of the helical coil on heat transfer of TFHE.

From Figure 7, nearly 297 % increment in helical coil inside Nusselt number is observed concerning increase in helical coil inside fluid volume flow rate from 1 LPM to 5 LPM. This considerable increment in helical coil inside Nusselt number is resulted mainly due to a significant increase in convective heat transfer coefficient for more produced fluid turbulence inside the helical coil. Similarly, nearly 2 % increment in helical coil outside fluid Nusselt number is observed concerning an increase in helical coil inside fluid volume flow rate from 1 LPM to 5 LPM (in Figure 7). This marginal increment in the helical coil outside the Nusselt number is observed due to the least changes in convective heat transfer coefficient for fluid flow outside of the helical coil as the volume flow rate and equivalent diameter are kept constant during the study.

Effect of Fluid Flow Rate at the Outer Side of the Helical Coil Heat Transfer

The heating performance. i.e. helical coil inside Nusselt number, Nu_{if} and outside Nusselt number, Nu_{of} of the current HEx are assessed for three different volume flow rates of helical coil outside fluid i.e. 3 LPM, 4 LPM and 5 LPM successively. The result of this study is represented graphically in Figure 8 for counterflow arrangement. It is ensured that the helical coil inside Nusselt number, Nu_{if} decreases negligibly, and outside Nusselt number, Nu_{of} increases considerably with the rise in fluid flow rate outside of the helical coil.

From Figure 8, a nearly 0.15% decrement in helical coil inside Nusselt number is observed concerning an increase in helical coil outside fluid volume flow rate from 3 LPM to 5 LPM. This negligible decrement in the helical coil inside Nusselt number is resulted due to a slight decrease in convective heat transfer coefficient for the constant fluid flow rate and tube diameter inside of the helical coil.
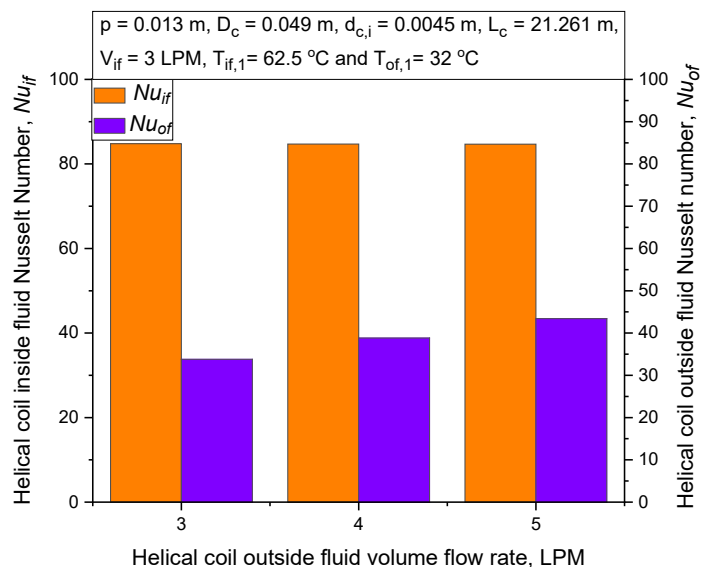

Figure 8. Effect of fluid flow rate outside helical coil on heat transfer of TFHE.

From Figure 8, a nearly 28.5% increment in helical coil outside fluid Nusselt number is observed concerning increase in helical coil outside fluid volume flow rate from 3 LPM to 5 LPM. This considerable increment in the helical coil outside Nusselt number is observed due to a significant increase in convective heat transfer coefficient for fluid flow outside of the helical coil with the rise in volume flow rate for constant equivalent diameter.

Effect of Fluid Temperature at the Inlet of the Helical Coil on Heat Transfer

The heating performance i.e. helical coil inside Nusselt number, Nu_{if} and outside Nusselt number, Nu_{of} are assessed for three different fluid temperatures at the inlet of helical coil, i.e. 40.4 ℃, 62.5 ℃, and 83.4 ℃ successively and elucidated in Figure 9. The Nusselt number for fluid flow inside and outside of the helical coil increases with the rise in fluid temperature at the inlet of the helical coil.
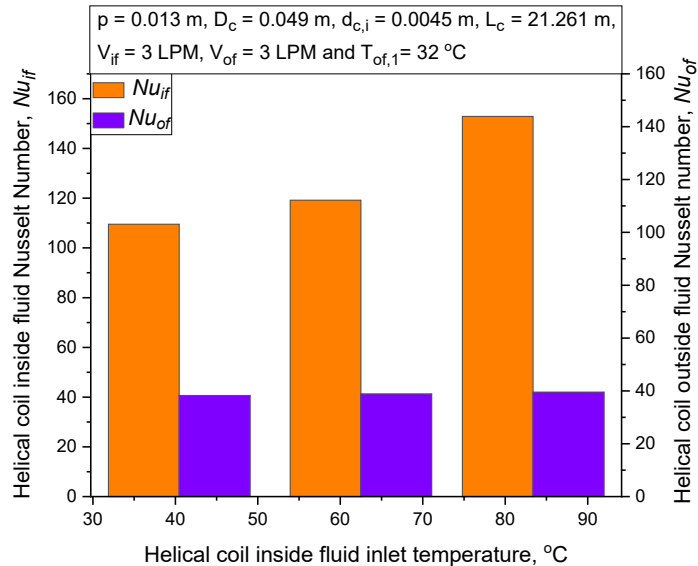

Figure 9. Effect of fluid inlet temperature inside of the helical coil on heat transfer of TFHE.

From Figure 9, nearly a 39.5 % increment in the helical coil inside the Nusselt number is observed concerning an increase in fluid inlet temperature inside the helical coil from 40.4 ℃ to 83.4℃. This considerable increment in helical coil inside Nusselt number results in a due rise in thermal conductivity and coefficient of convective heat transfer for a fixed tube diameter of the helical coil. Similarly, from Figure 9, nearly 3 % increment in helical coil outside fluid Nusselt number is observed concerning an increase in fluid inlet temperature inside of the helical coil from 40.4 ℃ to 80.3 ℃. This minimal increment in the helical coil outside Nusselt number is observed due to little increment in convective heat transfer coefficient for constant fluid flow rate, fluid inlet temperature, and equivalent diameter at the outer side of the helical coil.

Effect of Fluid Temperature at Shell Inlet on Heat Transfer

The heating performance, i.e. helical coil inside Nusselt number, Nu_{if} and outside Nusselt number, Nu_{of} of the current HEx are assessed for three disparate entry temperatures, 25 ℃, 32 ℃, and 39 ℃ successively outside of the helical coil and elucidated in Figure10. It is noticed in Figure 10 that the Nusselt number outside and inside the helical coil increases marginally with growth in inlet fluid temperature outside of the helical coil. Nearly 5% increment in helical coil inside Nusselt number is observed increasing in fluid inlet temperature at outside of the helical coil from 25℃ to 39℃. This minimal increment in helical coil inside Nusselt number results due to little rise in thermal conductivity and coefficient of convective heat transfer for a fixed tube diameter of the helical coil. Similarly, from Figure 10, nearly 4.5 % increment in helical coil outside fluid Nusselt number is observed concerning an increase in fluid inlet temperature at the outside of the helical coil from 25 ℃ to 39 ℃. This minimal increment in the helical coil outside Nusselt number is observed due to little increment in convective heat transfer coefficient for constant flow rate and equivalent diameter at the outer side of the helical coil.
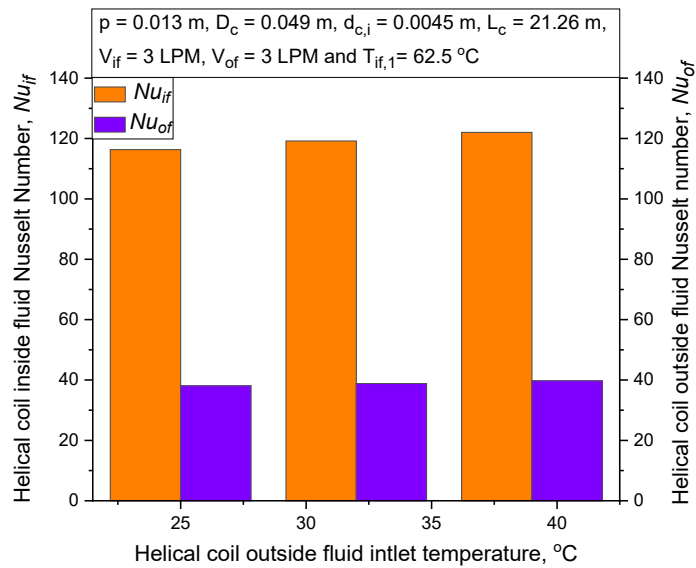
Figure 10. Effect of fluid inlet temperature at the outer side of the helical coil on heat transfer of TFHE.

Effect of Helical Coil Tube Diameter on Heat Transfer

The heating performance of the helical coil inside Nusselt number, Nu_{if}, and outside Nusselt number, Nu_{of} are evaluated for three different diameters of the helical coil tube; 0.004 m, 0.007 m, and 0.01 m successively and elucidated in Figure11. It is observed from Figure11 that the fluid flow Nusselt number inner side and outer side of the helical coil declines with the rise in helical tube diameter. Nearly 53.5 % decrement in helical coil inside Nusselt number is observed concerning increasing in helical coil tube diameter from 0.004 m to 0.01 m. This considerable decrement in helical coil inside Nusselt number is resulted due from a significant decrease in convective heat transfer coefficient for a reduction in corresponding flow velocity, Reynolds number. Similarly, nearly 38 % decrement in helical coil outside fluid Nusselt number is observed for increasing in helical coil tube diameter from 0.004 m to 0.01 m. This significant decrement in the helical coil outside the Nusselt number resulted due to a considerable decrease in a decrement in equivalent diameter outside of the helical coil.
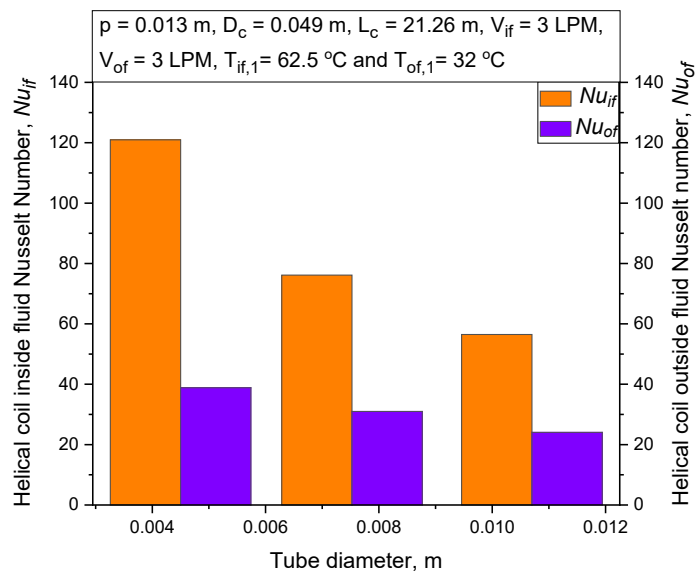

Figure 11. Effect of tube diameter of the helical coil on heat transfer of TFHE.

Effect of Coil Diameter of the Helical Tube on Heat Transfer

The heating performance of helical coil, inside Nusselt number, Nu_{if}, and outside Nusselt number, Nu_{of} are evaluated for three helical coil diameters of 0.042 m, 0.049 m, and 0.056 successively and elucidated in Figure12. It is observed in Figure12 that the Nusselt number for fluid flow inside helical coil negligibly increases and outside helical coil decreases with rising in coil diameter.
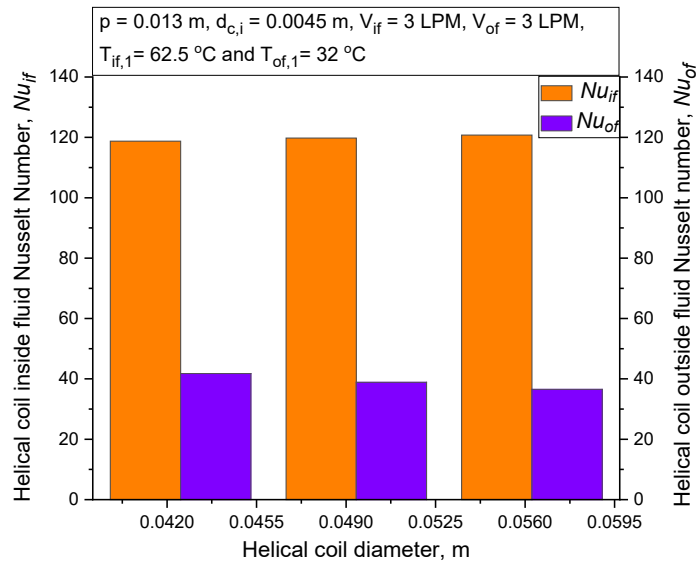
Figure12. Effect of the diameter of the helical coil on heat transfer of TFHE.

From Figure 12, nearly 1.5 % increment in helical coil inside Nusselt number is observed to increase in coil diameter of the helical coil tube from 0.042 m to 0.056 m. This negligible increment in helical coil inside Nusselt number is resulted due to the collective effect of an increase in convective heat transfer coefficient and decrease in thermal conductivity for increased heat transfer surface area of the helical coil.

From Figure 12, nearly 12.5 % decrement in helical coil outside fluid Nusselt number is observed concerning increase in coil diameter of the helical coil tube from 0.042 m to 0.056 m. This decrement in the helical coil outside Nusselt number is resulted due to decreased equivalent diameter at the outer side of the helical coil with increment in helical coil diameter.

Effect of the Pitch of Helical Coil on Heat Transfer

The heating performance i.e. helical coil inside Nusselt number, $Nu_{if,}$ and outside Nusselt number, Nu_{of} are evaluated for three helical coil pitches i.e. 0.013 m, 0.018 m, and 0.023 successively and elucidated in Figure13. It is observed in Figure13 that the helical coil inside the Nusselt number decreases and the helical coil outside the Nusselt number increase with the rise in coil pitch.

From Figure 13, nearly 3.5 % decrement in helical coil inside Nusselt number is observed to increase in helical coil pitch from 0.013 m to 0.023 m. This small decrement in helical coil inside Nusselt number is resulted due from a decrease in convective heat transfer coefficient for decreased number of turns of the helical coil.

From Figure 13, nearly 36 % increment in helical coil outside fluid Nusselt number is observed concerning increase in helical coil pitch from 0.013 m to 0.023 m. This significant increment in the helical coil outside the Nusselt number is resulted due to increased equivalent diameter at the outer side of the helical coil.
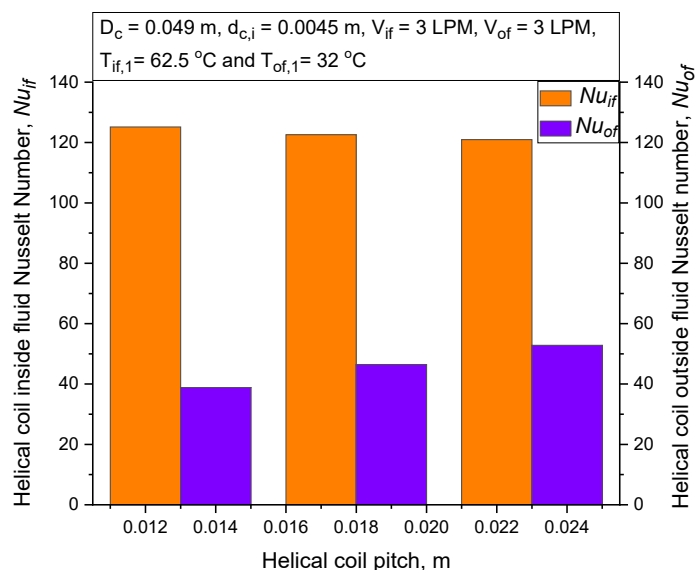

Figure13. Effect of helical coil pitch on heat transfer of TFHE.

DEVELOPMENT OF CORRELATION

TFHE heating performance is reliant on various factors and the influence of these factors on fluid Nusselt number for flow outside and inside helical coil is described in the above sections. From the literature review [19], it is identified that rate of fluid flow inside and outside helical coil, coil pitch as well as tube diameter have a substantial effect on the thermal performance of the fluid flow inside and outside of the helical coil.
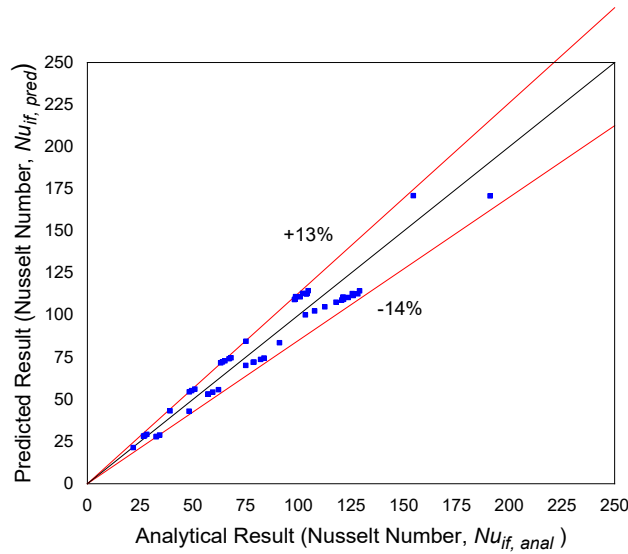

Figure 14. Comparison of analytical and predicted results for helical tube side flow.

In the present study, a total of 62 runs of performance measurement for the TFHE is carried out analytically for different fluid flow rates, tube diameter, coil pitch, and counterflow arrangement in both turbulent and laminar flow regimes. After that, the anticipated correlation of Nusselt number for fluid flow inside the helical coil is determined using log-linear regression analysis and communicated as:

$$Nu_{if} = 0.0176 Re_{if}{}^{0.821} Pr_{if}{}^{0.334} \left(\frac{d_{c,i}}{D_c}\right)^{0.025}, 3400 < Re_{if} < 48900, 0.091 < \left(\frac{d_{c,i}}{D_c}\right) < 0.216, 2.97 < Pr_{if} < 4.06 \tag{37}$$

Afterwards, the Nusselt number for fluid flow inside the helical coil is determined using Eq. (37) and compared with the theoretical results. In Figure 14, it is shown that good agreement among both results is observed within the +13% to -14% data range of the suggested correlation. Likewise, the Nusselt number for fluid flow outer side of the helical coil is calculated using log linear regression analysis and communicated as:

$$Nu_{of} = 2.272 . Re_{of}{}^{0.292} . Pr_{of}{}^{0.165} . \left(\frac{d_{c,i}}{D_c}\right)^{0.0029}, 280 < Re_{of} < 2750, 0.091 < \left(\frac{d_{c,i}}{D_c}\right) < 0.216, 3.6 < Pr_{of} < 5.2 \tag{38}$$

The Nusselt number for fluid flow outside the helical coil is determined using Eq. (38) and compared with the theoretical results. In Figure 15, it is shown that good agreement among both results is observed within +10% to -11% data range of the suggested correlation. In the above-stated correlations, it is observed that the influence of $\left(\frac{d_{c,i}}{D_c}\right)$ TFHE heating performance; i.e. Nusselt number inside and outside of the helical coil is negligible. Insufficient data toward correlation development may be a reason for this.
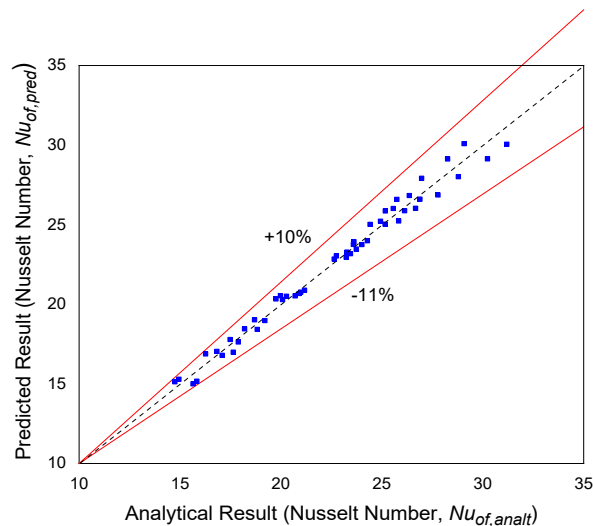
Figure 15. Comparison of analytical and predicted results for outer annulus side flow.

CONCLUSION

In this study**,** the heating performance of the TFHE was analytically investigated against certain design parameters, and new heat transfer correlations for the flow of fluid inside and outside of the helical coil of the present HEx were proposed. For the said requirement, the test section of the present Hex was modeled analytically, compared with literature, and validated against experimental temperature distribution data. From several design parameters, the rate of fluid flow, the temperature at the inlet, tube diameter, coil diameter, and coil pitch were the main parameters considered for this analysis. The outcomes of the current work can be briefed as follows.

i.   The Nusselt number for fluid flow inside the helical coil increases with the rise in the coil side volume flow rate, coil side fluid inlet temperature, coil outside fluid inlet temperature, and a coil diameter of the helical coil. The increment in coil side Nusselt number was calculated at nearly 297%, 39.5%, 5%, and 1.5% for the rise in coil side volume flow rate from 1 LPM to 3 LPM, coil side fluid inlet temperature from 40.4 °C to 83.4 °C, coil outside fluid inlet temperature from 25 °C to 39 °C, and a coil diameter of the helical coil from 0.042 m to 0.056 m respectively. The coil side flow rate and inlet temperature were detected as the two key parameters contributing maximum increment in coil side Nusselt number with 297% and 39.5% of the contribution.

ii.   The Nusselt number for fluid flow outside of the helical coil increases with the growth in coil side fluid flow rate and fluid inlet temperature, volume flow rate, and inlet temperature outside of the helical coil and helical coil pitch, respectively. The increment in coil outside Nusselt number was calculated at nearly 2%, 3%, 28.5%, 4.5%, and 36% for the rise in coil side volume flow rate from 1 LPM to 3 LPM, coil side fluid inlet temperature from 40.4 °C to 83.4 °C, coil outside fluid flowrate from 3 LPM to 5 LPM and inlet temperature from 25 °C to 39 °C, and coil pitch of the helical coil from 0.013 m to 0.023 m respectively. The coil pitch and fluid flow rate at the outside of the helical coil were detected as the two key parameters which contribute maximum increment in coil outside Nusselt number with 36% and 28.5% of the contribution.

iii. The Nusselt number for fluid flow inside of the helical coil decreases with a rise in volume flow rate outside of the coil, helical tube diameter, and helical coil pitch. The decrement in coil side Nusselt number was calculated nearly 0.15%, 53.5%, and 3.5% for the rise in volume flow rate outside of the coil from 3 LPM to 5 LPM, helical tube diameter from 0.004 m to 0.01 m, and helical coil pitch from 0.013 m to 0.023 m respectively. The helical tube diameter was detected as the key parameter contributing the maximum decrement in coil inside Nusselt number with 53.5% contribution.

iv.   The Nusselt number for fluid flow outside of the helical coil decreases with a rise in helical tube diameter and helical coil diameter. The decrement in coil outside Nusselt number was calculated at 38% and 12.5% for the rise in helical tube diameter from 0.004 m to 0.01 m and helical coil diameter from 0.042 m to 0.056 respectively. The helical tube diameter was detected as the key parameter contributing the maximum decrement in coil inside Nusselt number with 38% of the contribution.

v.   A new heat transfer correlation was proposed for turbulent fluid flow inside and outside of the helical coil of the TFHE. Predicted correlation outcomes were compared with the theoretical results. Decent agreement among both results was observed within the data range of +13% to -14% for coil side Nusselt number and +10% to -11% coil outside Nusselt number respectively.

vi.   More analytical data may be added to develop a more precise Nusselt number correlation for fluid flow inside and outside of the helical coil in TFHE. It is one of the future scopes of the present study.

vii. The performance analysis of the TFHE concerning variation in tube diameter of the outermost and inmost tube may be considered as one of the future scopes of this study.

ACKNOWLEDGEMENT

REFERENCES

[1] D.P. Sekulić and R.K. Shah, "Thermal design theory of three-fluid heat exchangers," *Adv. Heat Transf.,* vol. 26, no. C, pp. 219–328, 1995, doi: 10.1016/S0065-2717(08)70297-1.

[2] A. Ünal, "Theoretical analysis of triple concentric-tube heat exchangers Part 1: Mathematical modelling," *Int. Commun. Heat Mass Transf.,* vol. 25, no. 7, pp. 949–958, 1998, doi: 10.1016/S0735-1933(01)00231-7.

[3] A. Ünal, "Theoretical analysis of triple concentric-tube heat exchangers Part 2: Case studies,". *Int. J. Heat Mass Transfer*, vol. 28, no.2, pp. 243-256, 2001, doi: 10.1016/S0735-1933(01)00231-7.

[4] D. Shrivastava, and T. A. Ameel, "Three-fluid heat exchangers with three thermal communications. Part A: a general mathematical model," *Int. J. Heat Mass Transfer*, vol. 47, no. 17-18, pp. 3855-3865, 2004, doi: 10.1016/j.ijheatmasstransfer.2004.03.021.

[5] D. Shrivastava, and T. A. Ameel, "Three-fluid heat exchangers with three thermal communications. Part B: effectiveness evaluation." *Int. J. Heat MassTransf.*, vol. 47, no. 17-18, pp. 3867-3875, 2004, doi: 10.1016/j.ijheatmasstransfer.2004.03.020.

[6] P. K. Nema, and A. K. Datta, "Improved milk fouling simulation in a helical triple tube heat exchanger," *Int. J. Heat Mass Transf.,* vol. 49, no. 19-20, pp. 3360-3370, 2006, doi: 10.1016/j.ijheatmasstransfer.2006.03.021.

[7] T. Mohapatra, B. N. Padhi, and S. S. Sahoo, "Experimental investigation of convective heat transfer in an inserted coiled tube type three fluid heat exchanger," *Appl. Therm. Eng.*, Vol. 117, pp. 297-307, 2017, doi: 10.1016/j.applthermaleng.2017.02.023.

[8] T. Mohapatra, S. Ray, S.S. Sahoo, and B. N. Padhi, "Numerical study on heat transfer and pressure drop characteristics of fluid flow in an insterted coiled tube type three fluid heat echanger," *Heat Transf.-Asian Res.*, Vol. 48, No.4, pp.1440-1465, 2019, doi: 10.1002/htj.21440.

[9] T. Mohapatra, B. N. Padhi, and S.S. Sahoo, "Analytical investigation and performance optimization of a three fluid heat exchanger with helical coil insertion for simultaneous space heating and water heating," *Heat Mass Transf.,* Vol. 55, pp. 1723-1740, 2019. doi: 10.1007/s00231-018-02545-2.

[10] R. Kharat, N. Bhardwaj, and S. R. Jha, "Development of heat transfer coefficient correlation for concentric helical coil heat exchanger," *Int. J. Therm. Sci.*, Vol. 48, no. 12,pp. 2300-2308, 2009, doi: 10.1016/j.ijthermalsci.2009.04.008.

[11] J. Y. San, C. H. Hsu, and S. H. Chen, "Heat transfer characteristics of a helical heat exchanger," *Appl. Therm. Eng.*, vol. 39, pp. 114-120, 2012, doi: 10.1016/j.applthermaleng.2012.01.048.

[12] M. M. K. Bhuiya *et al.*, "Heat transfer enhancement and development of correlation for turbulent flow through a tube with triple-helical tape inserts," *Int. Commun. Heat Mass Transf.*, vol. 39, no. 1, pp. 94-101, 2012, doi: 10.1016/j.icheatmasstransfer.2011.09.007.

[13] A. Touatit, and C. Bougriou, "Optimal diameters of triple concentric-tube heat exchangers," *Int J Heat Tech..*, vol. 36, pp. 367-375, 2018, doi: doi.org/10.18280/ijht.360149.

[14] L. Jian-you, "Numerical and experimental investigation for heat transfer in triplex concentric tube with phase change material for thermal energy storage,". *Sol. Energy*, vol. 82, no. 11, pp. 977-985, 2008, doi: 10.1016/j.solener.2008.05.006.

[15] A. A. Al-Abidi *et al.*, "Numerical study of PCM solidification in a triplex tube heat exchanger with internal and external fins," *Int. J. Heat Mass Transf.,* vol. 61, pp. 684-695, 2013, doi: 10.1016/j.ijheatmasstransfer.2013.02.030.

[16] A.K.Tiwari *et al.*, "Experimental and numerical investigation on the thermal performance of triple tube heat exchanger equipped with different inserts with WO_3/water nanofluid under turbulent condition," *Int. J. Therm. Sci*., vol. 164, pp. 106861, 2021, doi: 10.1016/j.ijthermalsci.2021.106861.

[17] V. Krishna, P.G. Hegde, N. Subramanian, and K.N. Seetharamu, Effect of ambient heat-in-leak on the performance of a three fluid heat exchanger for cryogenic applications using finite element method," *Int. J. Heat Mass Transf.*, Vol. 55, pp. 5459–5470, 2012, doi: 10.1016/j.ijheatmasstransfer.2012.05.005.

[18] G.A. Quadira, I.A. Badruddin, and N.J. S. Ahmed, "Numerical investigation of the performance of a triple concentric pipe heat exchanger," *Int. J. Heat Mass Transf.*, vol. 75, pp. 165–172, 2014, doi: 10.1016/j.ijheatmasstransfer.2014.03.042.

[19] M. S. El-Genk, and T. M. Schriener, "A review and correlations for convection heat transfer and pressure losses in toroidal and helically coiled tubes," *Heat Transf. Eng.,* vol. 38, no. 5, pp 447-474. 2017, doi: 10.1080/01457632.2016.1194693.

[20] R. A. Seban, and E. F. McLaughlin, "Heat transfer in tube coils with laminar and turbulent flow,". *Int J Heat Mass Transf.*, vol. 6, pp.387–395, 1963, doi: 10.1016/0017-9310(63)90100-5.

[21] G. F. C. Rogers, and Y. R. Mayhew, "Heat transfer and pressure loss in helically coiled tubes with turbulent flow." *Int J Heat Mass Transf.*, vol. 7, pp. 1207-1216, 1964, doi: 10.1016/0017-9310(64)90062-6.

[22] E. F. Schmidt, "Heat transfer and pressure loss in spiral tubes." *Chem.-Ing.-Tech.*, vol. 39, pp. 781-789, 1967, doi: 10.1002/cite.330391302.

[23] T. L. Bergman, A. S. Lavine, F. P. Incropera, and D. P. DeWitt. *Intro. heat transf.,* John Wiley & Sons, 2011.

[24] R. K. Patil, B. W. Shende, and P. K. Ghosh, "Designing a helical-coil heat exchanger". *Chem. Engg.*, vol. 89, pp. 85-88, 1982.